LINKING THE HIGH-RESOLUTION ARCHITECTURE OF MODERN AND ANCIENT WAVE-DOMINATED DELTAS: PROCESSES, PRODUCTS AND FORCING FACTORS

R. Bruce Ainsworth[1], Boyan K. Vakarelov[2], Christian H. Eide[3], John A. Howell[4] and Julien Bourget[5]

[1] *Australian School of Petroleum, University of Adelaide, Adelaide, SA 5005, Australia*

[2] *SEDBASE OOD, 21B Moskovska Street, Sofia 1000, Bulgaria*

[3] *Department of Earth Science, University of Bergen, PO Box 7803, 5020 Bergen, Norway*

[4] *School of Geosciences, University of Aberdeen, Meston Building, Aberdeen, AB24 3UE, UK*

[5] *Centre for Energy Geoscience, School of Earth Sciences, University of Western Australia, Crawley, WA 6009, Australia*

ABSTRACT: Wave-dominated deltas are often fed by single trunk distributary channels which can remain the primary source of sediment supply to the delta for periods of thousands of years. Consequently, the sedimentary architecture of the delta can record subtle changes in sediment supply and wave intensity over significant periods of time. The geomorphological expression of these variations are beach-ridge elements and disconformity-bounded, beach-ridge element-sets. There are two types of beach-ridge element-sets observed on modern deltas, those associated with mouth-bar progradation (mouth-bar element sets), and those associated with delta-lobe flank accretion (lobe element-sets). When the ratio of the rate of sediment supply by the fluvial system (F) is relatively high with respect to the rate of sediment removal at the mouth-bar location by waves (W) (i.e., the F/W ratio is high), the mouth-bar element-sets are deposited. When the F/W ratio is low, sediment is preferentially transported to the lobe flanks and the lobe element-sets are deposited. The mouth-bar and lobe element-sets are bounded by the same unconformity and disconformity surfaces and are together termed element-set pairs. Analogous cyclical patterns of deposition have also been recognized in plan-view and vertical sections from

studies of ancient wave-dominated deltas from outcrop and subsurface data (seismic, well logs and cores).

Dating of beach-ridge elements on deltas deposited in the last 6000 years (Holocene) indicate a rate of formation of individual ridges in the order of decades to one-hundred years. The beach-ridge element-sets and beach-ridge element-set pairs are typically formed in periods of hundreds of years. Groups of beach-ridge element-sets, beach-ridge element-set pairs and associated genetically related distributary channel deposits form individual delta lobes. The delta lobes are generated by fluvial avulsion episodes which are autogenic events intrinsic to the fluvial deposystems, and which occur on the order of multiple hundreds to thousands of years. Individual beach-ridge element formation has previously been attributed to autogenic events. We propose that centennial-scale climate cycles may provide a mechanism for generating and controlling the intra-lobe changes in F/W ratio that generate the beach-ridge element-set and beach-ridge element-set-pair morphology of wave-dominated deltas. It follows that observations of such morphologies in the ancient may potentially be used as a proxy for subtle centennial-scale climatic forcing of wave-dominated deltas through deep geological time.

INTRODUCTION

Beach ridges are common geomorphological features on modern wave-dominated deltas and coastlines (Bhattacharya and Giosan, 2003) and have also been reported from the ancient (e.g. Jackson et al. 2010; Ainsworth et al. 2015). The genesis of these features has been the subject of debate over the past several decades (see summaries in Otvos, 2000 and Tamura, 2012). Individual ridges are thought to form by 1) progradation of sandy beach berms in relation to fairweather waves, 2) building of coarse-grained ridges by storm waves, or 3) welding of longshore bars onto the beach face (Tamura, 2012). The regular alternation of beach ridges and swales (Fig. 1) has led to speculation that their genesis may be related to cyclical external forcing factors (e.g. solar or climate cycles; Tamura, 2012). However, some authors argue this is unlikely given the variability in formative durations of individual beach ridges since some have decadal and others have centennial-scale durations (Sanjaume and Tolgensbakk, 2009). The grouping of ridges into disconformity-bounded beach-ridge sets is also a common feature on wave-dominated deltas and coastlines (Fig. 1). The bounding surfaces of beach-ridge sets are typically ascribed to reductions in sediment supply to the shoreline (Tamura, 2012) leading to coastal erosion by waves and the formation of beach ridge unconformity and disconformity surfaces. Renewed sedimentation results in the initiation of a new beach-ridge set (Tamura, 2012).

Cyclical groupings of depositional beds and bedsets, and stratal disconformities have also been described in vertical sections in ancient wave-dominated deltaic deposits (e.g. Hampson, 2000; Sømme et al., 2008). Some authors have attempted to relate these stratal units and disconformities to those observed in modern systems (Hampson and Storms, 2003; Storms and Hampson, 2005, Hampson et al., 2008; Sømme et al., 2008). Two-dimensional forward-modeling testing key uncertainties such as changes in sediment supply, wave power, and sea level (Storms and Hampson, 2005, Sømme et al., 2008; Charvin et al., 2011) have been able to replicate similar stratal geometries to those observed, and suggest that these processes individually, or in conjunction with each other, may be responsible for the formation of beach ridges and beach-ridge sets.

Recent advances in the classification of shallow marine systems (Ainsworth et al. 2011; Vakarelov and Ainsworth, 2013; Ainsworth et al. 2017) have enabled both modern and ancient architectural units from bed-scale up to deposystem-scale to be recognized and classified. This consistent classification enables direct cross-comparison of modern and ancient systems at the same architectural-unit scales (Table 1). This permits measured timeframes for architectural units from modern dated coastal systems (Carbon 14 [^{14}C] or optically stimulated luminescence

[OSL]; see examples in Tamura, 2012) to be applied as time duration estimates for the same stratigraphic units in ancient deposystems (c.f. Miall, 2015).

Rivers that supply the same wave-dominated delta lobe for hundreds to thousands of years (Fig. 1) provide a continuous record of sediment supply to the river mouth. This permits patterns or cycles in sediment supply that may exist on a decadal or centennial time-scale to be identified via mapping and dating of beach ridges and beach-ridge set bounding surfaces.

The key objectives of this paper are: 1) to compare the stratal patterns of beach ridges and beach-ridge sets in well-constrained and dated Holocene, wave-dominated, fluvial-influenced deltas (Wf classification of Ainsworth et al. 2011) with those from ancient Wf deltaic systems, and 2) to propose possible formative driving mechanisms for the cyclical changes in beach-ridge-set packaging to explain the observed stratal patterns. The genesis of non-deltaic, wave-dominated, beach-ridge strandplains are not considered in this paper.

ARCHITECTURAL OBSERVATIONS ON WAVE-DOMINATED DELTAS

Architectural Terminology for Comparing Modern and Ancient Systems

In order to provide a mechanism for identifying equivalent stratigraphic units from horizontal sections (usually satellite imagery of modern systems and high-resolution seismic attribute data from ancient systems) with the same architectural units in vertical sections (usually ancient systems in outcrop sections or modern and ancient systems in well logs and cores), Vakarelov and Ainsworth (2013) developed an architectural hierarchy called the *WAVE* classification (Table 1). Figure 2 details the horizontal (Figs. 2A, B) and vertical expression (Fig. 2C) of the architectural units pertinent to describing the level of detail observed in modern wave-dominated delta lobes (Fig. 1; Table 1). The individual wave-dominated delta lobe formed by a discrete fluvial avulsion is termed an element complex set (ECS; Figs. 1-2; Table 1; Vakarelov and Ainsworth, 2013; Ainsworth et al., 2017). The ECS is subdivided into elements (beach-ridge elements) and element sets (beach-ridge element-sets; Figs. 1-2; Table 1). There are two types of beach-ridge element-sets observed on the modern delta shown in Figure 1, those associated with mouth-bar progradation (mouth-bar element-sets; shaded green in Figs. 1-2; Table 1), and those associated with delta-lobe flank accretion (lobe element-sets; shaded orange in Figs. 1-2; Table 1). The two element-set types can be seen to regularly alternate close to the river mouth location and form mouth-bar and lobe element-set pairs which are bounded by erosional unconformities to non-depositional disconformities (Figs. 1-2). The unconformities are most easily observed at the river-mouth location and suggest periods where the ratio of the rate of sediment supply by the river (F) is relatively low with respect to the rate of sediment removal at the mouth-bar location by waves (W). That is, the F/W ratio is relatively low. The non-depositional disconformities form on the flanks of the delta in the lobe locations when deposition is primarily occurring on the mouth-bar at the river mouth during periods of high F/W (Figs. 1-2).

For completeness, the *WAVE* classification terminology for larger scale architectural units is also summarized in Table 1. Groups of ECS (delta lobes) generated by the same river are termed element-complex assemblages (ECA; equivalent to a modern-day, wave-dominated delta). The deposits of a regressive transit of deposystems (multiple coeval deltas) across a shelf are termed regressive element-complex-assemblage sets (RECAS). The overlying deposits of the transgressive transit of deposystems across the shelf are called transgressive element-complex-assemblage sets (TECAS). The composite regressive and transgressive stratigraphic-unit bounded by transgressive surfaces is the regressive-transgressive sequence (RTS). This level of hierarchy is the preferred level for the term “parasequence” (PS) when using the *WAVE* classification terminology (e.g. Ainsworth et al. 2018; this paper). The parasequence term is also used at this hierarchical level in the classical Book Cliffs papers (e.g. Hampson, 2000; Hampson et al. 2012).

Following Walther’s Law principles, it follows that architectural units recognized in plan views (beach-ridge elements, beach-ridge element-sets and delta lobes) should also have an equivalent expression in vertical sections (Table 1). Ainsworth et al. (2017) detailed the stacking patterns that define the different architectural units in vertical sections for different types of deltaic systems. Figure 2C illustrates that in symmetrical wave-dominated deltas, the beach-ridge elements are represented by bedsets (Table 1). Bedsets have been defined as a dm-to-m scale set of genetically related beds (Ainsworth et al. 2017). They can be arranged in an upward-thickening or upward-thinning trend. In normally prograding, wave-dominated systems, subsequent elements thicken-upward to form element-sets which are the vertical equivalent of beach-ridge-sets observed in plan-view (Table 1). Breaks in upward-thickening element trends define element-set boundaries. The element-sets themselves then thicken-upward to form element-complex sets (Fig. 2C). Breaks in upward-thickening element-set trends define element-complex-set boundaries (Ainsworth et al. 2017).

Holocene to Modern Wave-Dominated Deltas

The beach ridge and beach-ridge set architecture of Holocene to modern wave-dominated deltas are well illustrated by the Usumacinta–Grijalva Delta (Mexico; Fig. 1, Table 2). This delta has been the subject of detailed studies by numerous authors. See the recent paper by Nooren et al. (2017) and references therein for other relevant work. The current active lobe (ECS) of the delta initiated with the avulsion of the Usumacinta river circa 970 years before present (Fig.1; Nooren et al. 2017). The delta shows well developed beach ridges which group into beach-ridge sets around the mouths of the rivers (mouth-bar beach-ridge sets), and beach-ridge-sets away from the mouths of the river on the flanks of the delta in the lobe areas (lobe beach-ridge sets). The beach-ridge sets around the river mouth formed during periods of high fluvial discharge relative to the power of the waves to redistribute the sediment (high F/W time periods). Whilst the beach-ridge sets on the lobes formed during periods of low fluvial-discharge relative to the power of the waves to redistribute the sediment (low F/W time periods). Sediment was thus eroded from the mouth bar areas and transported to the lobe flanks in what is here termed the "lobe healing-phase" (Fig. 2A). The beach-ridge sets of the mouth bars (high F/W) and lobes (low F/W) are grouped together by unconformity and disconformity surfaces and form high and low F/W beach-ridge-set pairs (Figs. 1-2).

Ancient Wave-Dominated Deltas

The physical recognition of sub-aerial beach-ridge (element) and beach-ridge-set (element set) deposits in ancient progradational wave-dominated deltas is more challenging than for the Holocene deltas given the potential for the beach ridges (if originally present) to be removed during subsequent transgressive erosion events. The most convincing evidence of ancient beach-ridge deposits are examples from 3D seismic-attribute data which can provide images of plan-view sections through beach-ridge fields. An excellent example from the Jurassic of the North Sea is provided by Jackson et al. (2010). A higher-resolution seismic example which delineates beach ridges, high and low F/W beach-ridge-sets and beach-ridge-set pairs can be seen in Figure 3. This example is from the late Miocene, Bare Formation from the Northwest Shelf of Australia. See Sanchez et al. (2012) for details on the regional setting of the Bare Formation.

The link between the critical architectural units of a wave-dominated delta in plan-view (modern and seismic attribute data) and their vertical equivalents (well, core and outcrop data) is shown schematically in Figure 2 and from a real example in Figure 4 from a wave-dominated delta in the Eocene, Mangahewa Formation of the Taranaki Basin, New Zealand. See Higgs et al. (2012) for details on the regional setting of the Mangahewa Formation. Figure 4 shows an example of beach ridges in plan-view seismic-attribute data which are tied to vertical core and wireline log data which also exhibit the element and element-set cyclicity detailed in Figure 2. The beach ridges themselves are imaged on the seismic due to the peat accumulations in the shales between the ridges which exhibit as low impedance intervals on the seismic data.

There are relatively few reports of the physical expression of beach ridges being identified and described from outcrops. A notable exception is the interpreted beach ridge deposits from the Campanian of the Alberta Basin, Canada (Ainsworth et al. 2015). Since direct identification of the beach-ridge, beach-ridge-set and delta-lobe equivalents in vertical sections is challenging, recognition generally relies on the identification of architectural unit stacking patterns as defined in Figure 2C (c.f. Ainsworth et al. 2017).

The Blackhawk Formation and Star Point Sandstone of the Book Cliffs and Wasatch Plateau, Utah, USA comprises well documented extensive outcrops of Upper Cretaceous, wave-dominated deltaic systems (for a summary see Hampson and Howell, 2005). These well-studied outcrops provide an ideal location to examine vertical stacking patterns of stratal units deposited by wave-dominated deltas. An example from helicopter lidar derived virtual outcrops from the Sunnyside Member of the Blackhawk Formation, Book Cliffs, Utah is shown in Figure 5. See Sømme et al. (2008) and Eide et al. (2015) for a summary of the stratal architecture of the Sunnyside Member. The interpreted photo panel in Figure 5B illustrates the hierarchy of stratal packages from the smallest bedsets (elements), the groupings of upward-thickening elements into element sets, and the groupings of upward-thickening element-sets into element-complex sets. Breaks in upward-thickening trends define stratal unit boundaries. The element-complex sets stack vertically to form the parasequences.

The KSP010 parasequence of the Star Point Sandstone, Wasatch Plateau, Utah, USA (Eide et al. 2014) provides another example of the vertical stratal unit stacking hierarchy from a wave-dominated delta (Figs. 6, 7). This example also provides vertical detail from the mouth-bar to lobe transition area (Fig. 6) where the detailed onlap and downlap relationships of element-set-pairs can be observed directly adjacent to the distributary channel that fed the delta. The detailed vertical architecture of the lobe element-complex section of the parasequence is illustrated by bed-scale sedimentary logging (Fig. 7B) and comprises genetically related sandier and thickening-upward beds grouped into bedsets (elements). These elements are themselves grouped into sandier and thickening-upward genetically related units (element sets). The element sets then group into sandier and thickening-upward units (element complex sets). The element-complex-sets have been equated to deltaic lobe switching events (Eide et al. 2014; Ainsworth et al., 2017). This lobe switching relationship can also be observed in vertical section on the summary section derived from the helicopter lidar panel in Figure 7A.

DISCUSSION

Linking Modern and Ancient Wave-Dominated Deltas

Previous authors have attempted to link the cyclicity observed in wave-dominated deltas interpreted from outcrop logs to the cyclicity seen in modern wave-dominated delta systems (Hampson and Storms, 2003; Storms and Hampson, 2005, Hampson et al. 2008; Sømme et al. 2008; Charvin et al. 2010). However, no rules for identification of architectural units in vertical section were presented by these authors. The term "bedset" in the Blackhawk Formation, Utah, USA studies listed above has been equated to the avulsion body or delta lobe by some of the workers and this concurs with our interpretation of the element-complex set (Figs. 1-7; Table 1; Vakarelov and Ainsworth, 2013; Ainsworth et al. 2017). An advance presented here over the previous work is the recognition of two further levels of stratal unit hierarchy, at a scale below that of the delta lobe body (ECS): 1) the element ("bedset" *sensu* Ainsworth et al. 2017; Table 1) which is suggested to correspond to the "beach-ridge" observed in plan-view on modern delta systems (Figs. 1-2; Table 1) and on high-resolution seismic attribute data (Figs. 3-4), and 2) the element-set which is suggested to correspond to the "beach-ridge sets" (Table 1) observed in plan-view on modern systems (Fig. 1) and on high-resolution seismic attribute data (Fig. 3).

Figures 7C and 7D illustrate a model for linking the cyclicity observed on modern wave-dominated deltas (Fig. 1) with that observed on ancient deltas (Figs. 3-7). Breaks in the upward-thickening trends of elements define element-set boundaries and breaks in the upward thickening trends of element sets define element-complex-set boundaries (Ainsworth et al., 2017). This model also illustrates a fluvial avulsion event (Fig. 7C) which results in the deposition of a new delta lobe (ECS). In vertical section, the new delta lobe is recognized by the break in the expected upward-thickening stacking patterns of the element sets (Fig. 7D).

Depositional Rates

Towards the mouth of the river where the stratigraphic record is most sensitive to fluvial input rates, individual beds represent daily or seasonal activity (Table 3) whilst elements (individual beach-ridges and bedsets) represent the product of multiple storm and river flood events and can be initiated by decadal-scale fluvial-discharge cycles (Rodriguez et al. 2000) or fairweather progradation of beach berms (Tamura, 2012; Table 3). The genesis of the element-sets and element-set-pairs detailed from modern and ancient examples in this paper, have not been the subject of previous speculation or discussion. Carbon 14 and OSL dating of modern deltas (Fig. 1; Table 3) suggest that the element-set-pairs of mouth-bar beach-ridge sets and lobe beach-ridge sets, which are related to high and low F/W cycles respectively, occur on a centennial time-scale (Fig. 8; Table 3).

Further from the river mouth on the flanks of the delta lobes (e.g. see location ii on Fig. 1C), sediment accumulation rates are slower (only 2.5 km of progradation compared to 6.7 km of progradation at the river mouth on the Usumacinta-Grijalva Delta; Fig. 1), mouth-bar element sets are not deposited and there are also fewer beach ridges on the lobe than at the river mouth. These relationships are also detailed schematically in Figure 8. The obvious stratigraphic unconformities defining the element sets at the river mouth are less obvious at the lobe locations and in some places appear concordant with older strata (disconformities). The result of this is that there are fewer beach ridges on the lobe flanks representing the same number of beach ridges and the same amount of time at the river mouth (Fig. 8C). That is, if beach ridge duration is calculated by dividing the time taken for deposition by the number of beach ridges (a common method for estimating beach-ridge durations), then individual beach ridges on the lobes appear to represent greater amounts of time than beach ridges at the river mouth (Fig. 8C). However, in the case of wave-dominated deltas, this apparent mismatch in beach-ridge duration calculations is likely to be a function of the time sequestered in the unconformities and disconformities (Fig. 8D, E) rather than being due to significant differences in the actual time taken to deposit an individual beach ridge.

The Impact of Real World Delta Complexity

The models detailed in Figures 7C, 7D and 8 represent the simplest form of a symmetric wave-dominated delta wherein all the sediment supplied to the delta is delivered by the river and redistributed at the river mouth by waves. In the case of the Usumacinta–Grijalva Delta (Fig. 1), sediment supply to the delta through the trunk distributary channel was basically uninterrupted for the past circa 970 years (Nooren et al. 2017). In other Wf symmetrical deltas such as the Jequitinhonha Delta (Brazil) constant sediment supply was not maintained along the axis of the one trunk distributary channel for the duration of the current delta lobe (ECS; Fig. 9, Table 2). The Jequitinhonha Delta has previously been described by Dominguez et al. (1983, 1987) and Martin et al. (1983). It is currently undergoing forced regression (Martin et al. 2003; Dias and Kjerfve, 2013). The active lobe of the Jequitinhonha delta initiated with the avulsion of the Jequitinhonha river circa 2,500 years before present (Fig. 9; Martin et al. 1993). The current delta lobe at the river mouth location has prograded 8 km in the last 2,500 years (Fig. 9C). The geomorphology of the delta suggests that during this time the main channel has also diverted to the north for periods of time and then back to the current distributary channel location (Fig. 9C). This may indicate that the count of element-set pairs along the main distributary channel (Fig. 9C; Table 2) is incomplete and may represent a minimum number.

In many modern deltas, sediment is also supplied to the system from other sources apart from the deltaic distributary-channels, namely by longshore-transport mechanisms. Some deltas exhibit a strong degree of longshore sediment-supply. See Bhattacharya and Giosan (2003) for a summary of the impact of out-of-plane longshore sediment transport on delta morphology. Consequently, the models proposed herein would require modification to account for varying degrees of longshore transport supplying sediment to the delta from sources external to the deltas own distributary channel(s).

The Paraiba do Sul Delta (Brazil) (Fig. 10, Table 2) is a well-documented asymmetrical Wf delta and has been the subject of work by multiple previous authors (e.g. Dominguez et al. 1983, 1987; Martin et al. 1985, 1993, 2003; Da Rocha, 2013; Vasconcelos et al. 2015). For the past 5,000 years it has been undergoing forced regression (Martin et al. 1985, 1993, 2003; Dias and Kjerfve, 2013). The current active lobe of the Paraiba do Sul delta initiated with the avulsion of the Paraiba do Sul river. The timing of this event varies depending on the type of age dating method utilized (Table 2). Martin et al. (1993) using ^{14}C methods date the avulsion at circa 2,500 years before present. However, Vasconcelos et al. (2016) using OSL methods date the avulsion at circa 1,300 years before present. The current delta lobe at the river mouth location has thus prograded 11 km in the last 1,300 to 2,500 years (Fig. 10C). In this example, there is no representation of mouth bar deposits on the updrift side of the delta since the mouth-bars are deflected downdrift by longshore currents. However, the updrift part of the delta, the lobe EC is still segmented into an active mouth-bar progradation phase of beach ridges (high F/W) and a delta-lobe healing phase (low F/W) as per the deposits of the symmetric deltas of the Usumacinta–Grijalva and Jequitinhonha Deltas detailed in Figures 1 and 9 respectively. In the Paraiba do Sul Delta, both the high and low F/W lobe element-sets are accreting due to sediment supplied from older eroding delta lobes to the south (Fig. 10).

Note that the asymmetrical Paraiba do Sul delta has high and low F/W element-set pairs formed on the same centennial scale cyclicity as observed for the high and low F/W element-set pairs on the symmetrical deltas of the Usumacinta–Grijalva and Jequitinhonha (Table 2).

Potential Forcing Mechanism of Centennial-Scale Stratigraphic Cycles

The data discussed above suggests that beach-ridge element-sets near the river mouths of wave-dominated deltas represent periods of high F/W (Fig. 8D), and the beach ridge element-sets on the down-flank lobes represent delta-lobe healing during periods of low F/W (Fig. 8E). Together, the high and low F/W beach-ridge element-sets form beach-ridge element-set pairs. The erosional unconformities and disconformities that separate the element-set pairs are diachronous, occurring in different locations at different times during a high to low F/W cycle (Figs. 8D, E). The element-set pairs are deposited on a centennial timescale, i.e., in the order of 100 to 200 years (Table 2; Fig. 8). The repetitive changes in the F/W ratio required to form the element set pairs is a product of either regularly fluctuating sediment discharge from the river and/or regularly alternating wave energy.

The centennial-scale cyclicity forming the high and low F/W element-set pairs, that occurs over periods of thousands of years, from the three different modern deltas illustrated in this paper (Table 2), suggests that a regular external forcing factor could be responsible for producing this cyclicity. Possible centennial-scale climatic variations influencing precipitation rates have been postulated using modeling studies by Karnauskas et al. (2012). Greenland temperature records and lake levels in north-eastern USA have also been shown to illustrate centennial-scale climatic variability through the Holocene (Fawcett et al. 2011; Newby et al., 2014) as have sea surface temperatures in the early Holocene record of the Gulf of Mexico (LoDico et al. 2006). The studies of Thirumalai et al. (2018) are particularly relevant to the current ECS of the Usumacinta–Grijalva Delta on the Gulf of Mexico which was initiated approximately 1,000 years ago (Fig. 1, Table 2. These authors reconstructed sea surface temperatures and salinity in the Gulf of Mexico over the past 1,000 years. Their results showed a marked centennial scale occurrence of sea surface temperature and salinity variations which they correlated to widespread precipitation anomalies on adjacent continents.

Wave-dominated deltas with relatively small drainage basins (Table 2), and single distributary channels located in the same position at the coastline for thousands of years (Figs. 1, 9, 10) would be extremely sensitive to precipitation variations in their catchments; i.e., the effect will be greatly amplified due to water and sediment discharge funneling to one point, the single terminal distributary channel. These types of deltas would perhaps be expected to be an efficient vehicle for recording subtle sediment discharge changes related to precipitation variations responding to centennial-scale climatic cycles. Using flume-tank modeling studies, Van Saparoea and Postma (2008) concluded that "…high-resolution stratigraphy in the delta-realm to be controlled by high frequency (climate) changes in (river) discharge". The simplest and most straightforward explanation in this case is that it is more likely that climate-driven precipitation changes are responsible for the repeated changes in F/W that drive the consistent patterns of element-set pairs (Figs. 1 and 8-10) rather than climate-driven changes in wave power. However, with the data currently available, the additional impact of climate-driven changes in wave power cannot be dismissed.

Given our stratigraphic architectural observations and those of previous depositional and climate modeling studies, it is thus suggested that there is a case for the internal element-set-pair scale morphology of wave-dominated delta lobes to be controlled by centennial-scale climate cycles and that in turn, observations of beach-ridge-set delta morphology in the ancient may be used as a potential proxy for centennial-scale climate forcing in deep geological time.

Further Work

Further detailed work on dating the beach-ridge-set architectures described in this paper on a greater number of Holocene to modern, wave-dominated deltaic systems may help to elucidate the potential for the centennial-scale climate control mechanisms proposed herein.

This paper only addresses beach-ridge stratigraphic unit architectures on wave-dominated deltas. Other wave-dominated depositional settings such as non-deltaic, beach or strandplain systems exhibit similar beach-ridge stratigraphic architectures (beach ridges and beach-ridge sets). However, the lack of a direct sediment input point (the river), and the relatively low rates of sediment supply experienced by these systems compared to directly river-fed deltaic systems, results in a potential different subaerial and subsurface expression of the stratigraphic units. These wave-dominated, non-deltaic depositional settings require further work.

The influence of tides on the architecture of wave-dominated deltas with respect to their ability to record high and low F/W deposits also requires further consideration.

CONCLUSIONS

1) River mouths in wave-dominated delta settings are very sensitive to fluvial discharge and sediment supply variations. Supply variability is recorded in the stratigraphic record via beach ridges in mouth-bar and lobe settings (elements), mouth-bar and lobe beach-ridge sets (element sets), and beach-ridge-set-pairs which comprise mouth-bar beach-ridge-sets and lobe beach-ridge -sets.

2) The beach-ridge-set pairs reflect periods of high F/W (mouth-bar beach-ridge element-sets) and low F/W (lobe beach-ridge element-sets). They are delineated by erosional unconformities and disconformities.

3) All these architectural features can be recognized in both modern and ancient wave-dominated deltas via plan-view stratal mapping of beach ridges from satellite imagery or high-resolution seismic attribute data, and in vertical section by application of stacking pattern rules to stratal units (elements, element sets and element-complex sets).

4) The centennial-scale recurrence of high and low F/W element-set pairs observed near long-lived (1,000 to 2,500 years), Holocene, wave-dominated delta river-mouths are suggestive of an external forcing mechanism to drive the cyclicity.

5) It is proposed that centennial-scale climate cycles may well provide the external control on the internal morphology of wave-dominated deltas and thus that observations of beach-ridge

element-set and element-set-pair morphology on ancient deltas may be used as a potential proxy for centennial-scale climate forcing in deep geological time. However, further work is required on detailed dating of beach-ridge sets on more modern wave-dominated deltas to expand the dataset available for substantiating this hypothesis.

ACKNOWLEDGMENTS

Many thoughts and concepts used in this paper were initially developed as a result of work conducted with funding provided to the *WAVE* Consortium at the Australian School of Petroleum, University of Adelaide (RBA, BKV and JB). The consortium sponsors (Apache, BAPETCO, BHPBP, BG, BP, Chevron, ConocoPhillips, Nexen, OMV, Shell, Statoil, Todd Energy, and Woodside Energy) are thus thanked for making this work possible. We are indebted to journal reviewers Cornel Olariu and Howard Feldman, and to associate editor Janok Bhattacharya for numerous comments and suggestions that improved the clarity of the manuscript.

REFERENCES

AINSWORTH, R.B. 1994, Marginal marine sedimentology and high-resolution sequence analysis: Bearpaw - Horseshoe Canyon transition, Drumheller, Alberta: Bulletin of Canadian Petroleum Geology, v. 42, p. 26-54.

AINSWORTH, R.B., VAKARELOV, B.K., AND NANSON, R.A., 2011, Dynamic spatial and temporal prediction of changes in depositional processes on clastic shorelines: Toward improved subsurface uncertainty reduction and management: American Association of Petroleum Geologists, Bulletin, v. 95, p. 267-297.

AINSWORTH, R.B., VAKARELOV, B.K., LEE, C., MACEACHERN, J.A., MONTGOMERY, A.E., RICCI, L.P., AND DASHTGARD, S.E., 2015, Architecture and evolution of a regressive, tideinfluenced marginal marine succession, Drumheller, Alberta, Canada: Journal of Sedimentary Research, v. 85, p. 596-625, dx.doi.org/10.2110/jsr.2015.33.

Ainsworth, R.B., Vakarelov, B.K., MacEachern, J.A., Nanson, R.A., Lane, T.I, Rarity, F. and Dashtgard, S.E., 2016. Process-Driven Architectural Variability in Mouth-Bar Deposits: A Case Study from a Mixed-Process Mouth-Bar Complex, Drumheller, Alberta, Canada: Journal of Sedimentary Research, v. 86, p. 512-541. DOI: http://dx.doi.org/10.2110/jsr.2016:23

Ainsworth, R.B., Vakarelov, B.K., MacEachern, J.A., Rarity, F., Lane, T.I., and Nanson, R.A., 2017, Anatomy of a shoreline regression: implications for the high-resolution stratigraphic architecture of deltas: Journal of Sedimentary Research, v. 87, p. 425-459, doi: http://dx.doi.org/10.2110/jsr.2017.26

Ainsworth, R.B., McArthur, J.B. Lang, S.C., and Vonk, A.J., 2018. Quantitative sequence stratigraphy: AAPG Bulletin, v. 102, in press. doi:10.1306/02201817271

Bhattacharya, J.P., and Walker, R.G., 1992, Facies and facies successions in river- and wave-dominated depositional systems of the Upper Cretaceous Dunvegan Formation, northwestern Alberta: Bulletin of Canadian Petroleum Geology, v. 39, p. 165-191.

Bhattacharya, J.P., and Giosan, L., 2003, Wave-influenced deltas: geomorphological implications for facies reconstruction: Sedimentology, v. 50, p. 187-210.

Charvin, K., Hampson, G. J., Gallagher, K. l., and Labourdette, R., 2010, Intra-parasequence architecture of an interpreted asymmetrical wave-dominated delta: Sedimentology, v. 57, p. 760–785.

Charvin, K., Hampson, G.J., Gallagher, K.L., Storms, J.E.A., and Labourdette, R., 2011, Characterization of controls on high-resolution stratigraphic architecture in wave-dominated shoreface–shelf parasequences using inverse numerical modelling: Journal of Sedimentary Research, v. 81, p. 562–578.

DOMINGUEZ, J.M.L., BITTENCOURT, A.C.S.P., AND MARTIN, L.M., 1983, O papel da deriva litoranea de sedimentos arenosos na construcao das planicies costeiras associadas as desembocaduras dos rios Sao Francisco (SE-AL), Jequitinhonha (BA), Doce (ES), e Paraiba do Sul (RJ): Revista Brasileira de Geosciencias, v. 13, p. 98-105.

DOMINGUEZ, J.M.L., MARTIN, L.M., AND BITTENCOURT, A.C.S.P., 1987, Sea-level and quaternary evolution of river mouth-associated beach ridge plains along the east-southeast Brazilian Coast: A summary, in Nummedal, D., Pilkey, O.H., and Howard, J.D., eds., Sea-level Fluctuation and Coastal Evolution: SEPM, Special Publication 41, p. 115-127.

EIDE, C.H., HOWELL, J.A., AND BUCKLEY, S., 2014, Distribution of discontinuous mudstone beds within wave-dominated shallow-marine deposits: Star Point Sandstone and Blackhawk Formation, Eastern Utah: AAPG Bulletin, v. 98, p. 1401-1429.

EIDE, C.H., HOWELL, J.A. AND BUCKLEY, S.J., 2015, Sedimentology and reservoir properties of tabular and erosive offshore transition deposits in wave-dominated, shallow-marine strata: Book Cliffs, USA. Petroleum Geoscience v. 21, p. 55-73.

FAWCETT, P. J., WERNE, J.P., ANDERSON. R.S., HEIKOOP, J.M., BROWN, E.T, BERKE, M.A., SMITH, S.J., GOFF, F., DONOHOO-HURLEY, L., CISNEROS-DOZAL, L.M., SCHOUTEN, S., SINNINGHE DAMSTE, J.S., HUANG, Y., TONEY, J., FESSENDEN, J., WOLDEGABRIEL, G., ATUDOREI, V., GEISSMAN J.W. AND ALLEN, C. D., 2011, Extended megadroughts in the southwestern United States during Pleistocene interglacials: Nature, v. 470 (7335), p. 518–521.

FRAZIER, D.E., 1967, Recent deltaic deposits of the Mississippi River: Their development and chronology: Gulf Coast Association of Geological Societies, Transactions, v. XVII, p. 287-315.

HAMPSON, G.J., 2000, Discontinuity surfaces, clinoforms, and facies architecture in a wave-dominated shoreface-shelf parasequence: Journal of Sedimentary Research, v. 70, p. 325-340.

HAMPSON, G.J., AND STORMS, J.E.A., 2003, Geomorphological and sequence stratigraphic variability in wave-dominated, shoreface–shelf parasequences: Sedimentology, v. 50, p. 667–701.

HAMPSON, G.J. AND HOWELL, J.A., 2005, Sedimentologic and geomorphic characterization of ancient wave-dominated deltaic shorelines: examples from the Late Cretaceous Blackhawk Formation, Book Cliffs, Utah, in Bhattacharya, J.P. and Giosan, L., eds., River Deltas: Concepts, Models, and Examples: SEPM, Special Publication 83, p. 133–154.

HAMPSON, G.J., RODRIGUEZ, A.B., STORMS, J.E.A., JOHNSON, H.D., AND MEYER, C.T., 2008, Geomorphology and high-resolution stratigraphy of progradational wave-dominated shoreline deposits: Impact on reservoir-scale facies architecture, *in* Hampson, G.J., Steel, R.J., Burgess, P.M. and Dalrymple, R.W., eds., Recent Advances in Models of Siliciclastic Shallow-Marine Stratigraphy: SEPM, Special Publication 90, p. 117–142.

HIGGS, K.E, KING, P.R., RAINE, J.I., SYKES, R., BROWNE, G.H., CROUCH, E.M., BAUR, J.R., 2012, Sequence stratigraphy and controls on reservoir sandstone distribution in an Eocene marginal marine-coastal plain fairway, Taranaki Basin, New Zealand: Marine and Petroleum Geology, v. 32, p. 110-137.

JACKSON, C.A.L., GRUNHAGEN, H., HOWELL, J.A., LARSEN, A.L., ANDERSSON, A, BOEN, F., AND GROTH, A., 2010, 3D seismic imaging of lower delta-plain beach ridges: lower Brent Group, northern North Sea: Journal of the Geological Society, London, v. 167, p. 1225–1236. doi: 10.1144/0016-76492010-053.

KARNAUSKAS, K.B., SMERDON, J.E., SEAGER, R., AND GONZALEZ-ROUCO, J.F., 2012, A Pacific centennial oscillation predicted by coupled GCMs: Journal of Climate, v. 25, p. 5943-5961. DOI: 10.1175/JCLI-D-11-00421.1.

LODICO, J.M., FLOWER, B.P., AND QUINN, T.M., 2006, Subcentennial-scale climatic and hydrologic variability in the Gulf of Mexico during the early Holocene: Paleoceanography, v. 21, PA3015, doi:10.1029/2005PA001243.

MARTIN, L.M., DOMINGUEZ, J.M.L., AND BITTENCOURT, A.C.S.P., 1985, Roundness in Holocene sands of the Paraiba do Sul coastal plain, Rio de Janeiro, Brazil: Journal of Coastal Research, v. 1, p. 343-351.

MARTIN, L., SUGUIO, K., AND FLEXOR, J.M., 1993, As flutuaçoes de nivel do mar durante o Quaternario superior e a evoluçao geológica de "deltas" brasileiros: Boletim IG/ USP, 15, 1-186.

MARTIN, L.M., DOMINGUEZ, J.M.L., AND BITTENCOURT, A.C.S.P., 2003, Fluctuating Holocene Sea Levels in Eastern and Southeastern Brazil: Evidence from Multiple Fossil and Geometric Indicators: Journal of Coastal Research, v. 19, p. 101-124.

MIALL, A., 2015, Updating uniformitarianism: Stratigraphy as just a set of 'frozen accidents', *in* Smith, D.G., Bailey, R.J., Burgess, P.M., and Fraser, A.J., eds., Strata and Time: Probing the Gaps in Our Understanding: Geological Society of London, Special Publication 404, p. 11–36. http://dx.doi.org/10.1144/SP404.4

MITCHUM, R.M. Jr., and J.C. VAN WAGONER, 1991, High-frequency sequences and their stacking patterns: sequence-stratigraphic evidence of high-frequency eustatic cycles: Sedimentary Geology, v. 70, p. 131-160.

NEWBY, P.E., SHUMAN, B.N., DONNELLY, J.P., KARNAUSKAS, K.B., AND MARSICEK, J., 2014, Centennial-to-millennial hydrologic trends and variability along the North Atlantic Coast, USA, during the Holocene: Geophysical Research Letters, v. 41, p. 4300–4307, doi:10.1002/ 2014GL060183.

Nooren, K., Hoek, W.Z., Winkels, T., Huizinga, A, van der plicht, H., van dam, R.L., van Heteren, S., van Bergen, M.J., Prins, M.A., Reimann, T., Wallinga, J., Cohen, K.M., Minderhoud, P., and Middelkoop, H., 2017, The Usumacinta–Grijalva beach-ridge plain in southern Mexico: a high-resolution archive of river discharge and precipitation: Earth Surface Dynamics, v. 5, p. 529-556.

Otvos, E.G., 2000, Beach ridges - definitions and significance: Geomorphology, v. 32, p. 83-108.

Pattison, S.A.J., 1995, Sequence stratigraphic significance of sharp-based lowstand shoreface deposits, Kenilworth Member, Book Cliffs, Utah: American Association of Petroleum Geologists Bulletin, v. 79, p. 444-462.

Rodriguez, A.B., Hamilton, M.D., and Andersonn, J.B., 2000, Facies and evolution of the modern Brazos Delta, Texas: Wave versus flood influence: Journal of Sedimentary Research, v. 70, p. 283-295.

Sanchez C.M., Fulthorpe, C.S., and Steel, R.J., 2012, Middle Miocene–Pliocene siliciclastic influx across a carbonate shelf and influence of deltaic sedimentation on shelf construction, Northern Carnarvon Basin, Northwest Shelf of Australia: Basin Research, v. 24, p. 664-682, DOI: 10.1111/j.1365-2117.2012.00546.x

Sanjaume, E., and Tolgensbakk, J., 2009, Beach ridges from the Varanger Peninsula (Arctic Norwegian coast): Characteristics and significance: Geomorphology, v. 104, p. 82-92.

Sømme, T.O., Howell, J.A., and Hampson, G.J., and Storms, J.E.A., 2008, Genesis, architecture, and numerical modeling of intra-parasequence discontinuity surfaces in wave-dominated deltaic deposits: Upper Cretaceous Sunnyside Member, Blackhawk Formation, Book Cliffs, Utah, U.S.A., in Hampson, G.J., Steel, R.J., Burgess, P.M., and Dalrymple, R.W., eds., Recent Advances in Models of Shallow-Marine Stratigraphy: SEPM, Special Publication 90, p. 421-441.

STORMS, J.E.A., AND HAMPSON, G.J., 2005, Mechanisms for forming discontinuity surfaces within shoreface-shelf parasequences: Sea level, sediment supply or wave regime?: Journal of Sedimentary Research, v. 75, p. 67–81, doi: 10.2110/jsr.2005.007.

TAMURA, T., 2012, Beach ridges and prograded beach deposits as palaeoenvironment records: Earth-Science Reviews, v. 114, p.279-297.

TAYLOR, D.R., and LOVELL, R.W.W., 1995, High-frequency sequence stratigraphy and paleogeography of the Kenilworth Member, Blackhawk Formation, Book Cliffs, Utah, U.S.A., in Van Wagoner, J.C. and Bertram, G.T., eds., Sequence Stratigraphy of Foreland Basin Deposits: American Association of Petroleum Geologists, Memoir 64, p. 257-275.

THIRUMALAI, K., QUINN, T.M., OKUMURA, Y., RICHEY, J.N., PARTIN, J.W., POORE, R.Z., AND MORENO-CHAMARRO, E., 2018, Pronounced centennial-scale Atlantic Ocean climate variability correlated with Western Hemisphere hydroclimate: Nature Communications (2018) 9392, DOI: 10.1038/s41467-018-02846-4.

VAKARELOV, B.K., AND AINSWORTH, R.B., 2013, A hierarchical approach to architectural classification in marginal marine systems – bridging the gap between sedimentology and sequence stratigraphy: American Association of Petroleum Geologists Bulletin, v. 97, p. 1121-1161.

VAN SAPAROEA, A.P.H.V.D.B., AND POSTMA, G., 2008, Control of climate change on the yield of river systems, in Hampson, G.J., Steel, R.J., Burgess, P.M., and Dalrymple, R.W., eds., Recent Advances in Models of Shallow-Marine Stratigraphy: SEPM, Special Publication 90, p. 15-33.

VAN WAGONER, J.C., 1995, Sequence stratigraphy and marine to nonmarine facies architecture of foreland basin strata, Book Cliffs, Utah, U.S.A., in Van Wagoner, J.C., and Bertram, G.T., eds., Sequence Stratigraphy of Foreland Basin Deposits: American Association of Petroleum Geologists, Memoir 64, p. 137-223.

VASCONCELOS, S.C., ABUCHACRA, R.C., ROCHA, T.B. AND FERNANDEZ, G.B., 2016, Análise comparativa dos padrões morfoestratigráficos em deltas assimétricos, exemplo do delta do Rio Paraíba do Sul (RJ): XI SINAGEO - Simpósio Nacional de Geomorfologia - UGB - União da Geomorfologia Brasileira, 7 p. http://www.sinageo.org.br/2016/trabalhos/7/76061739.html

FIGURE CAPTIONS

FIG. 1. A) Location map for the Usumacinta–Grijalva Delta, Mexico. B) Location map for the current symmetrical delta lobe (element complex set; ECS). C) Detailed stratigraphic architecture depicting beach-ridge elements and beach-ridge sets (element sets; ES). Note the mouth-bar ES units (high F/W) combine with the lobe ES units (low F/W) to form ES pairs. D) Inset map showing detail of element-set pairs. E) Bathymetric contours of the current mouth-bar area interpreted from data supplied by Navionics (https://www.navionics.com/aus/apps/navionics-boating). An element complex (EC) is the equivalent of a facies association (Table 1; Vakarelov and Ainsworth, 2013). Base maps from Google Earth. Interpretation from *WAVE* Knowledgebase 3 (https://sedbase.com).

FIG. 2. Symmetrical wave-dominated delta architectural summary. A) High order architectural units; elements, element sets and element-set pairs. B) Intermediate order architectural units. Groupings of lower order units into element complexes (similar to facies associations). Mouth bar and lobe element-complexes illustrated. C) Sedimentary log cross-section illustrating vertical expression of architectural units shown in plan views in parts A) and B). See Table 1, the text and Vakarelov and Ainsworth (2013) for more detailed explanations and definitions of architectural units.

FIG. 3. A) Random seismic line cross section in two-way time (TWT) across the Bare Formation, Northwest Shelf, Australia (Middle Miocene to Pliocene). Location of seismic line X-Y shown on map (B). B) Route mean square (RMS) amplitude attribute map of seismic horizon in (A). Red and orange colors correspond to higher RMS amplitudes, white colors to lower RMS amplitudes. The map shows a north to north-north-west prograding wave-dominated delta fed by small fluvial systems. Wide areas of higher RMS amplitudes are interpreted as lagoon or lake settings (L) where dolomites, dolomitized sandstones and calcarenites have accumulated (Sanchez et al. 2012). Areas associated in map view with linear, sub-parallel geometries are interpreted as beach ridges (BR). C) Rio Coco partial analog from the Honduras and Guatemala border region. Interpretation from WAVE Knowledgebase 3 (https://sedbase.com). D) and E) Inset map (see part B) of RGB-color blending of spectral decomposition frequency attributes at 13, 36 and 57 Hertz. Compare the stratigraphic architectures with those observed on the Holocene delta in Figure 1 and summary Figure 2.

FIG. 4. Wave-dominated delta, Mangahewa Formation, Eocene, New Zealand. An example of ancient beach-ridges shown in plan-view (right) on a 3D seismic-attribute map (minimum acoustic impedance, 10 millisecond time window). The low impedance events (gray colors) in the south-east of the area are present day coals which would be related to swamp conditions at the time of deposition. The contrast between the low impedance coals in the beach-ridge swales with the beach ridges themselves enables visualization of the beach ridge geometries. The equivalent interval of the seismic attribute map is shown for two wells, one with core (POS-01) and one with gamma ray (GR) wireline data (POS-01B). Note the stratigraphic architecture at element, element-set and element-complex-set scales described in Fig. 2C is also recognizable in these deposits. ts = transgressive surface; tse = transgressive surface of erosion; mfs = maximum flooding surface. All surfaces are fifth order (10^4 to 10^5 years).

FIG. 5. Outcrop lidar photo panel showing a depositional strike section of the wave-dominated delta-lobe deposits of the Sunnyside Member of the Blackhawk Formation, Utah, USA (Sømme et al. 2008). These strata are exposed on the west side of the Beckwith Plateau, 15 km NW of the town of Green River (UTM coordinates; 12S 564092 4327978). S2 = Sunnyside parasequence 2 and S3 = Sunnyside parasequence 3. S2.5, S2.6, S3.1 and S3.2 are previously interpreted intra-parasequence "bedsets" (Sømme et al. 2008; Table 1). These stratigraphic units are the equivalent of the element complex set (ECS; Figs. 1, 2 and 4). Note that there are two further levels of hierarchy recognized at a smaller scale, element set (ES) and element (E). Compare with the measured sedimentological logs and wireline data shown in Figs. 4 and 7.

FIG. 6. A) Uninterpreted outcrop photo panel of the KSP010 wave-dominated delta parasequence of the Star Point Sandstone, Wasatch Plateau, USA. B) Interpreted photo panel showing bed or bedset terminations and downlaps (mouth-bar clinoform terminations) onto element-set boundaries and onlaps (lobe lateral-onlap onto the older mouth-bars) onto element-set-pair boundaries respectively. The mouth bar and lobe interpretations are from Eide et al. (2014). See Fig. 7A for interpreted lidar panel of the same interval and Fig. 7B for a measured sedimentary log. C) Model of idealized element-set pair transitions (taken from Fig. 2). Compare with the onlap and downlap geometries observed in the outcrop. Center of the distributary channel in part B) is at UTM coordinates 12S 487910 4338830.

FIG. 7. A) Outcrop lidar interpreted panel of the KSP010 wave-dominated delta parasequence of the Star Point Sandstone, Wasatch Plateau, USA. Note the hummocky morphology shown at top left which may be representative of beach-ridge deposits. See the photo panel of a portion of the outcrop around the distributary channel and mouth bar in Fig. 6. B) Sedimentary log from a location adjacent to the cross-section in A. Note the element, element set and element-complex-set architecture. A and B are both modified from Eide et al. (2014). C) and D) Depositional model to reconcile the stratigraphic architecture observed on modern symmetrical wave-

dominated deltas (Fig. 1) and ancient wave-dominated deltas (Figs. 3-7). Stratal units are identified by simple rules: Element sets (ES) are defined by upward-thickening elements (E; bedsets). Element complex sets (ECS) are formed by upward-thickening element sets. Regressive element complex assemblage sets (RECAS; regressive systems tract) are formed by thickening-upward element complex sets (see part B). Stratal unit boundaries are defined by breaks in these thickening-upward trends.

FIG. 8. Impact of the ratio of *rate of fluvial sediment supply* to *rate of longshore wave transport* (F/W) on symmetrical wave-dominated deltas. A) Formation of mouth-bar element set (ES) during high F/W. B) Subsequent formation of the lobe element-set "healing phase" during low F/W and hence the element-set pair. C) Repeated ES pairs form the delta lobe (element complex set; ECS). D) and E) illustrate the changes in F/W ratio through time at two depositional dip locations in part C). Note the out-of-phase deposition of the mouth bar ES and the lobe ES. Also note the diachroneity of the element-set-pair boundary unconformity and disconformity formation in C). Also note the assumption in D) and E) that the time duration for mouth-bar element-set and lobe element-set deposition are equal.

FIG. 9. A) Location map for the Jequitinhonha delta, Brazil. B) Location map for the current symmetrical delta lobe (element complex set; ECS). C) Detailed stratigraphic architecture depicting beach-ridge elements, beach-ridge sets (element sets; ES) and element-set pairs. The mouth-bar ES units are equivalent to the high F/W phases of the delta. The low F/W phases of the delta are represented by the healing phase lobe ES. Note the area to the north of the distributary channel where geomorphology is difficult to interpret due to the intermittent northerly migration of the distributary channel through this area. D) Bathymetric contours of the current mouth-bar area interpreted from data supplied by Navionics (https://www.navionics.com/aus/apps/navionics-boating). Note that the contours of the mouth-bar on the north and south sides of the river mouth mimic the geometry of the high F/W mouth-

bar element-sets. An element complex (EC) is the equivalent of a facies association (Table 1; Vakarelov and Ainsworth, 2013). Base maps from Google Earth. Interpretation from *WAVE* Knowledgebase 3 (https://sedbase.com).

FIG. 10. A) Location map for the Paraiba do Sul Delta, Brazil. B) Location map for the current asymmetrical delta lobe (element complex set; ECS). C) Detailed stratigraphic architecture depicting beach-ridge elements, beach-ridge sets (element sets; ES) and element-set pairs. Note that the mouth-bar element-complex is deflected in a downdrift direction hence on the updrift flank, lobe ES units rather than mouth-bar ES units (Figs. 1 and 8) represent the high F/W periods. The low F/W lobe ES units on the flanks represent the lobe healing phase and they combine with the high F/W lobe ES units to form element-set pairs. D) Bathymetric contours of the current mouth-bar area interpreted from data supplied by Navionics (https://www.navionics.com/aus/apps/navionics-boating). Note that the contours of the mouth-bar on the updrift side of the river mouth (right side) mimic the geometry of the updrift high F/W lobe element-sets in C). An element complex (EC) is the equivalent of a facies association (Table 1; Vakarelov and Ainsworth, 2013). The uncertainty in the age of the current ECS is due to different age dating techniques (Table 2). Base maps from Google Earth. Interpretation from *WAVE* Knowledgebase 3 (https://sedbase.com).

TABLE CAPTIONS

TABLE 1. Comparison of WAVE Classification terms for both plan and vertical section stratigraphic units relevant to wave-dominated deltas (Vakarelov and Ainsworth, 2013; Ainsworth et al. 2017) with commonly used geomorphological terms for plan views and stratigraphic terms for vertical sections (see Figures 2 and 7). Note that many of the stratigraphic units have no common geomorphological term (column 2; NA = not applicable) or vertical section stratigraphic term (column 3) making correlation of plan view geometries to vertical

section geometries problematical and prone to terminological misunderstandings and errors. Also note the common and confusing use of the terms “bedset”, “parasequence” and “parasequence set” at two to three different vertical hierarchical scales (columns 3 and 4). The WAVE Classification (column 1) provides a consistent and coherent language for comparing plan section and vertical section stratigraphic architectures. Abbreviations of WAVE terms are shown in italics at the end of the descriptions in column 1.

TABLE 2. Data for three Holocene delta lobes (element complex sets; ECS). Note the duration of element set (ES) pairs for each delta is estimated at around 100 to 200 years. Data for the Paraiba do Sul from Martin et al. (1993) and Vasconcelos et al. (2016), the Jequitinhonha delta from Martin et al. (1993), and the Usumacinta–Grijalva delta from Nooren et al. (2017). ^{14}C = Carbon 14 absolute dating methods. OSL = optically stimulated luminescence absolute dating methods. N.B. absolute age durations have an uncertainty associated with the measurements (see details in relevant sources), hence they are stated as approximate durations (c. = circa).

TABLE 3. Description, probable timeframe of deposition and formative mechanism for architectural units on wave-dominated deltas.

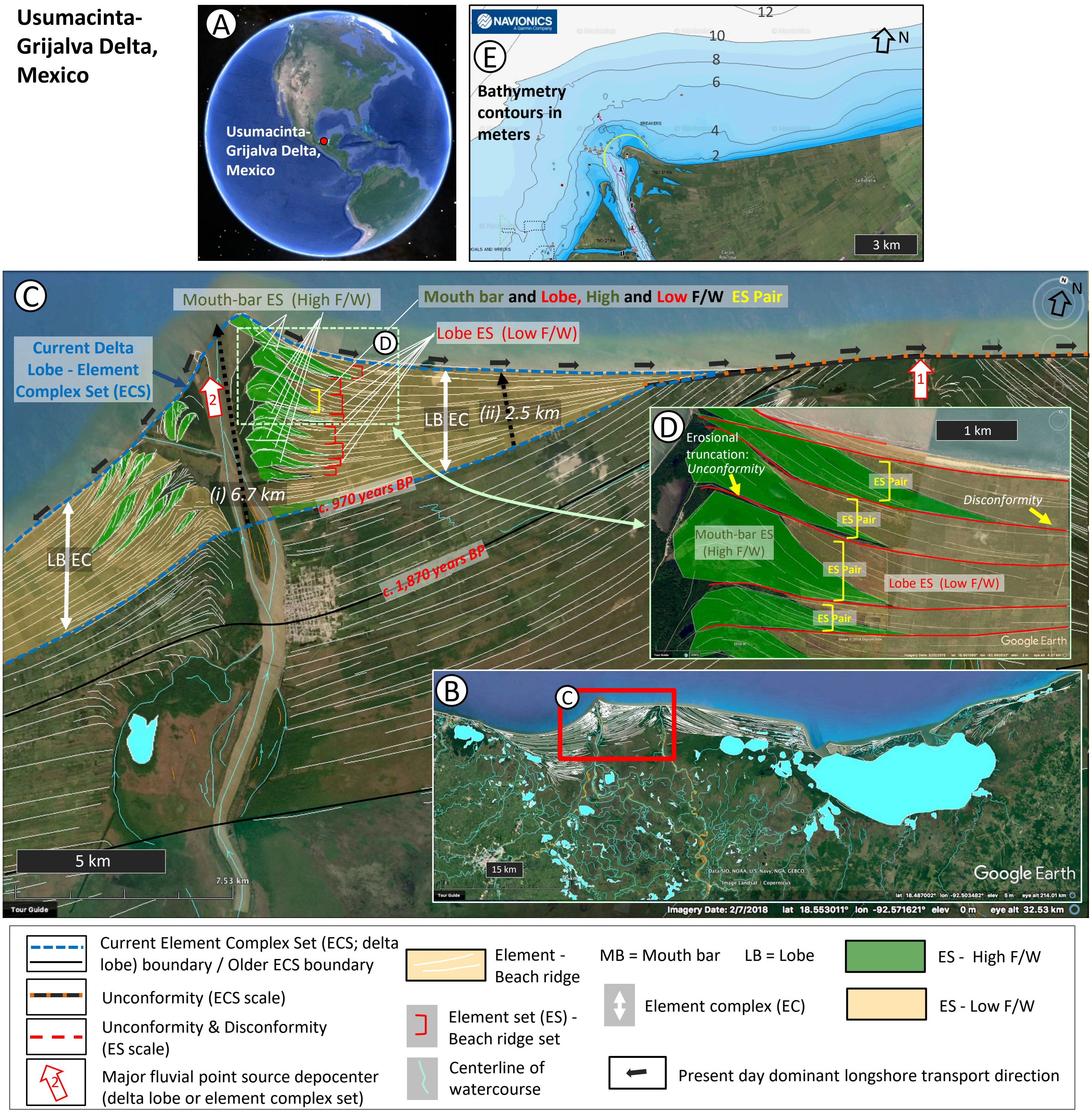
Usumacinta-Grijalva Delta, Mexico
A
Usumacinta-Grijalva Delta, Mexico
E
NAVIONICS
Bathymetry contours in meters
12
10
8
6
4
2
N
3 km
C
Mouth-bar ES (High F/W)
Mouth bar and Lobe, High and Low F/W ES Pair
Lobe ES (Low F/W)
Current Delta Lobe - Element Complex Set (ECS)
D
LB EC
(ii) 2.5 km
(i) 6.7 km
c. 970 years BP
c. 1,870 years BP
LB EC
5 km
1
2
D
Erosional truncation: Unconformity
1 km
ES Pair
Disconformity
Mouth-bar ES (High F/W)
Lobe ES (Low F/W)
B
C
15 km
Google Earth
Imagery Date: 2/7/2018 lat 18.553011° lon -92.571621° elev 0 m eye alt 32.53 km
Current Element Complex Set (ECS; delta lobe) boundary / Older ECS boundary
Unconformity (ECS scale)
Unconformity & Disconformity (ES scale)
Major fluvial point source depocenter (delta lobe or element complex set)
Element - Beach ridge
Element set (ES) - Beach ridge set
Centerline of watercourse
MB = Mouth bar
LB = Lobe
Element complex (EC)
Present day dominant longshore transport direction
ES - High F/W
ES - Low F/W

Fig. 1

Ainsworth et al. (2018)

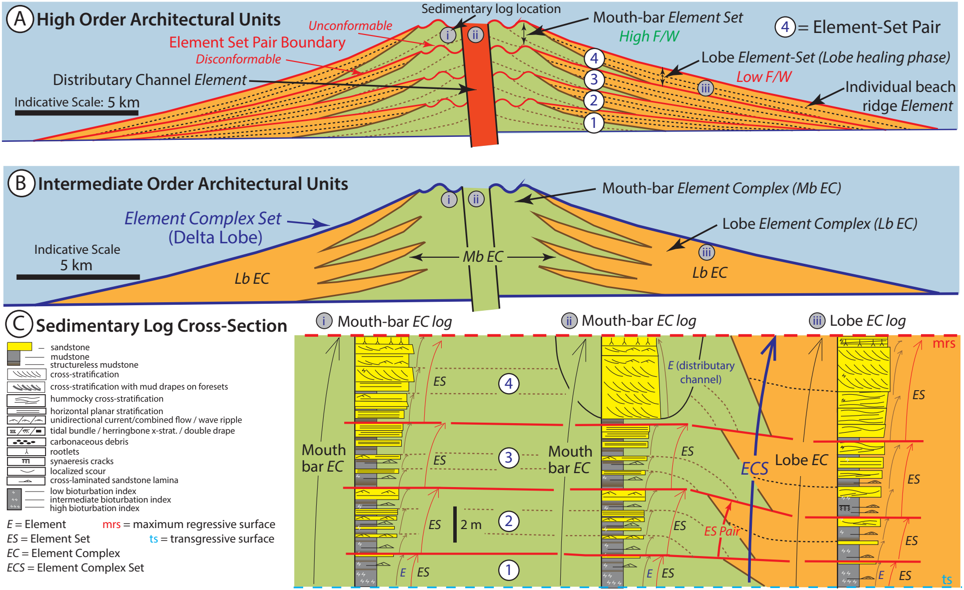

Fig. 2

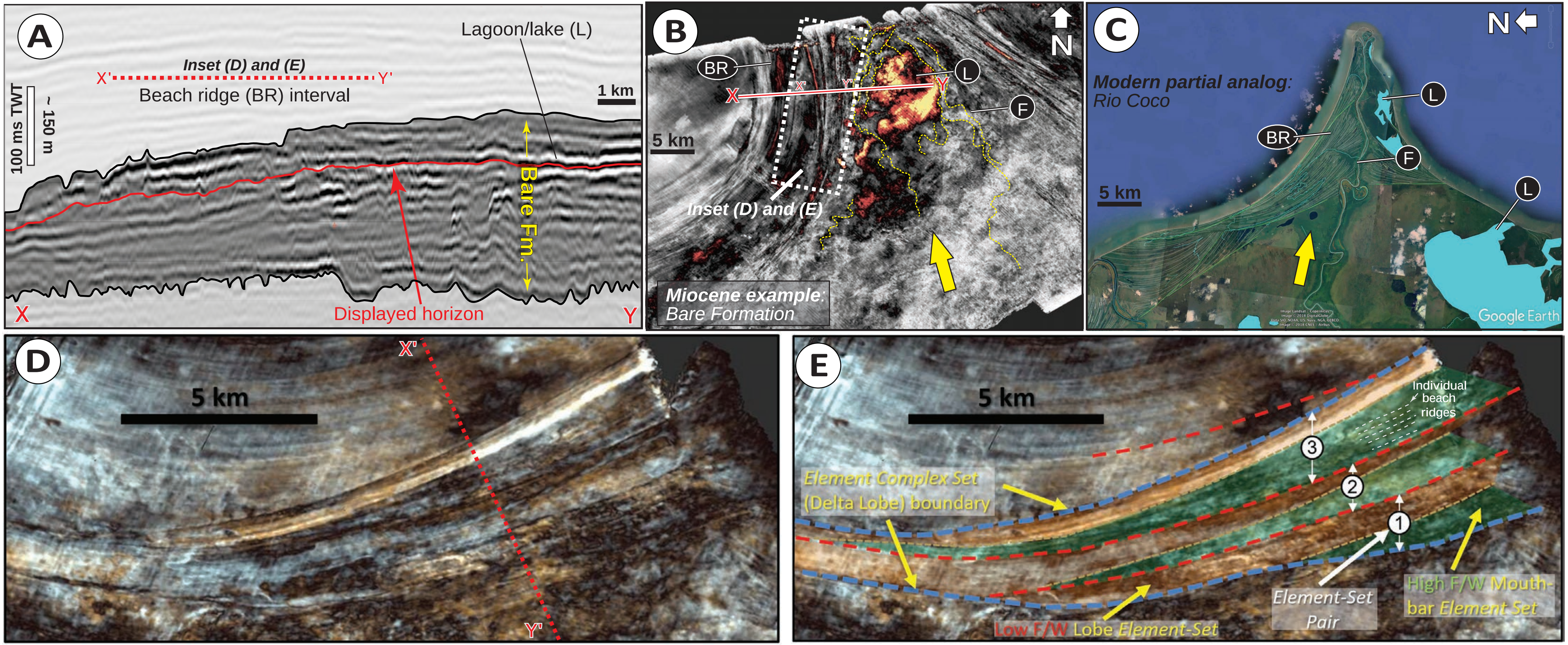
A
Lagoon/lake (L)
Inset (D) and (E)
X' Y'
Beach ridge (BR) interval
1 km
100 ms TWT
~ 150 m
Bare Fm.
X
Displayed horizon
Y
B
N
BR
X
X'
Y'
Y
L
F
5 km
Inset (D) and (E)
Miocene example:
Bare Formation
C
N
Modern partial analog:
Rio Coco
L
BR
F
5 km
L
Google Earth
D
X'
5 km
Y'
E
5 km
Individual beach ridges
3
2
1
Element Complex Set (Delta Lobe) boundary
Low F/W Lobe Element-Set
Element-Set Pair
High F/W Mouth-bar Element Set

Fig. 3

Ainsworth et al. (2018)

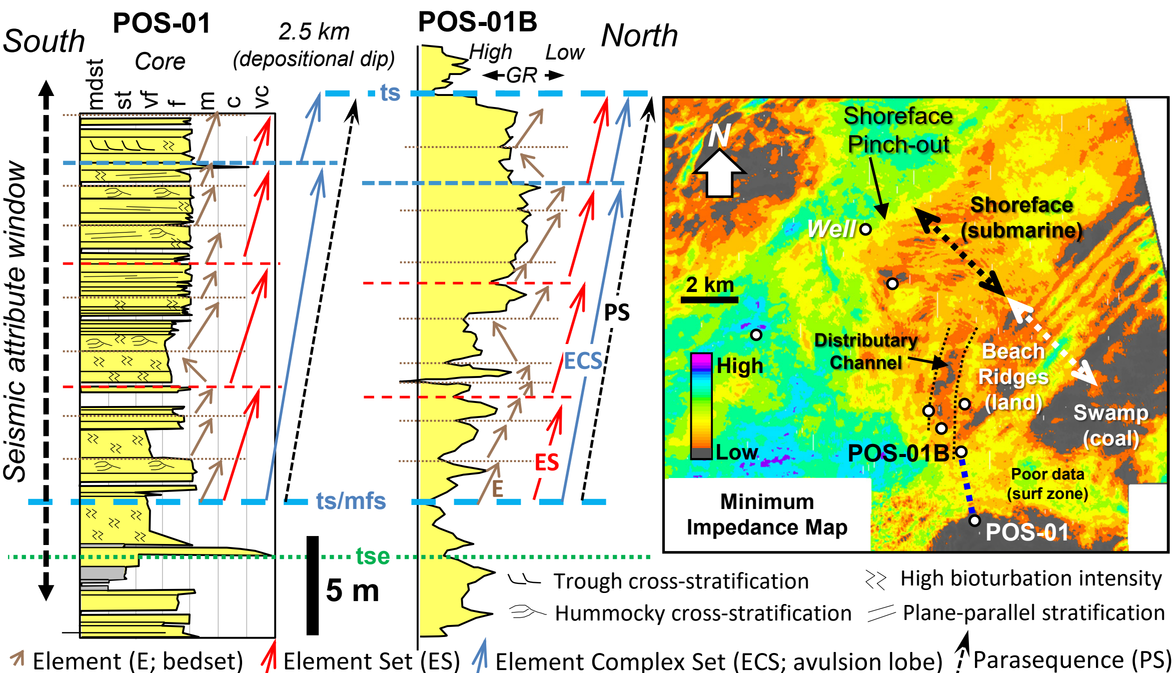

Fig. 4

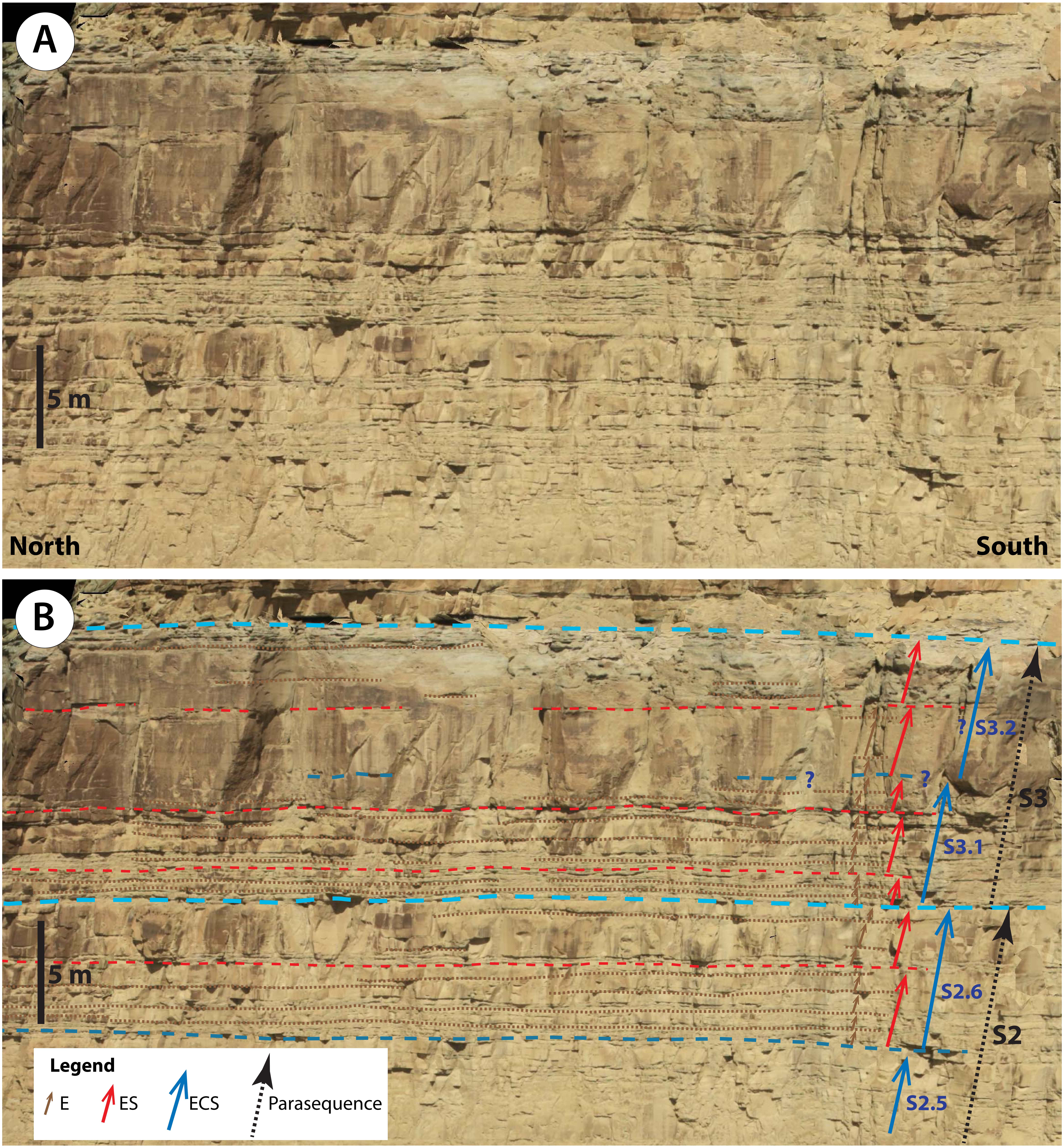
A
5 m
North
South
B
5 m
S3.2
?
?
?
S3
S3.1
S2.6
S2
S2.5
Legend
E
ES
ECS
Parasequence

Fig. 5

Ainsworth et al. (2018)

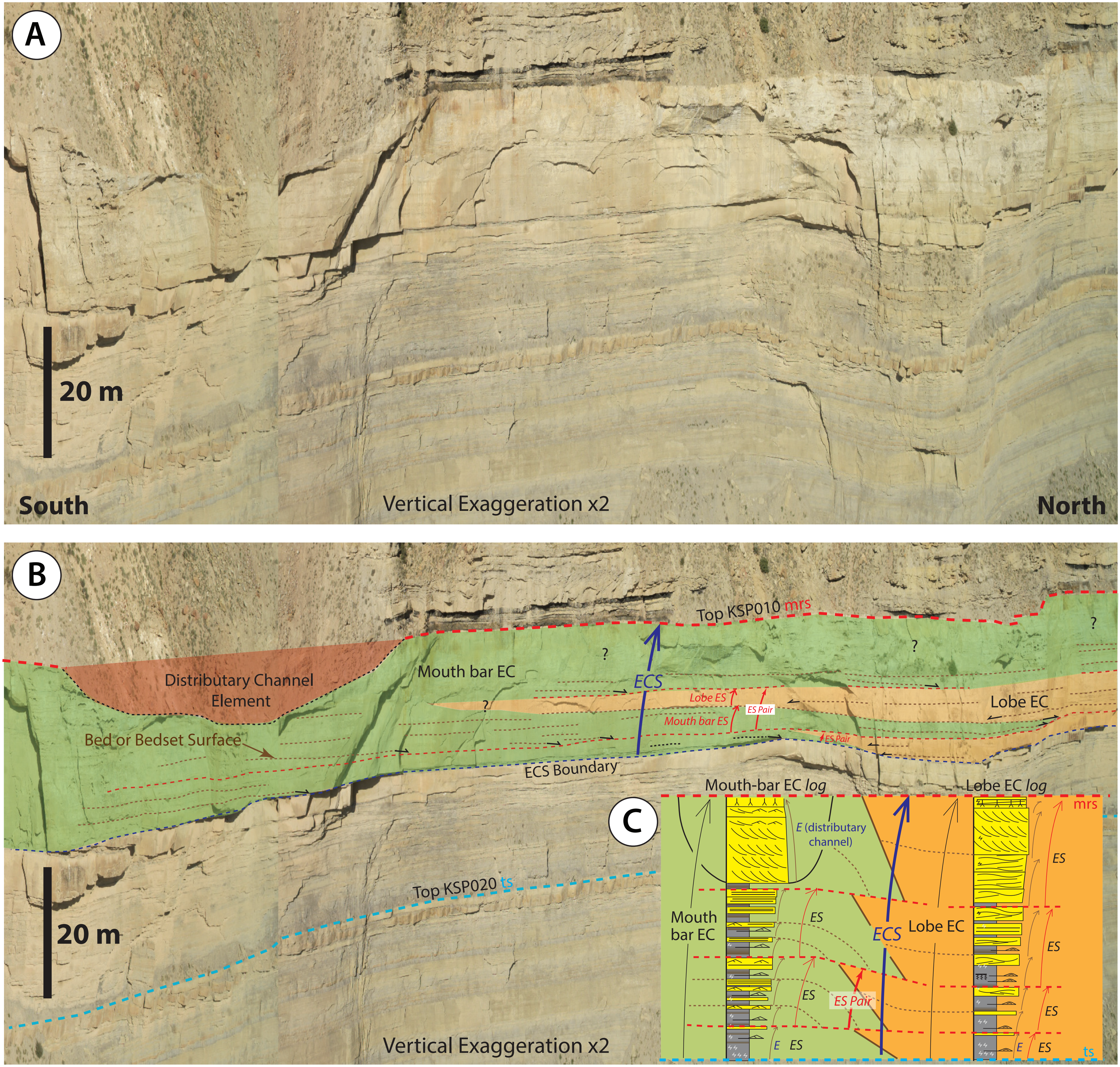

Fig. 6

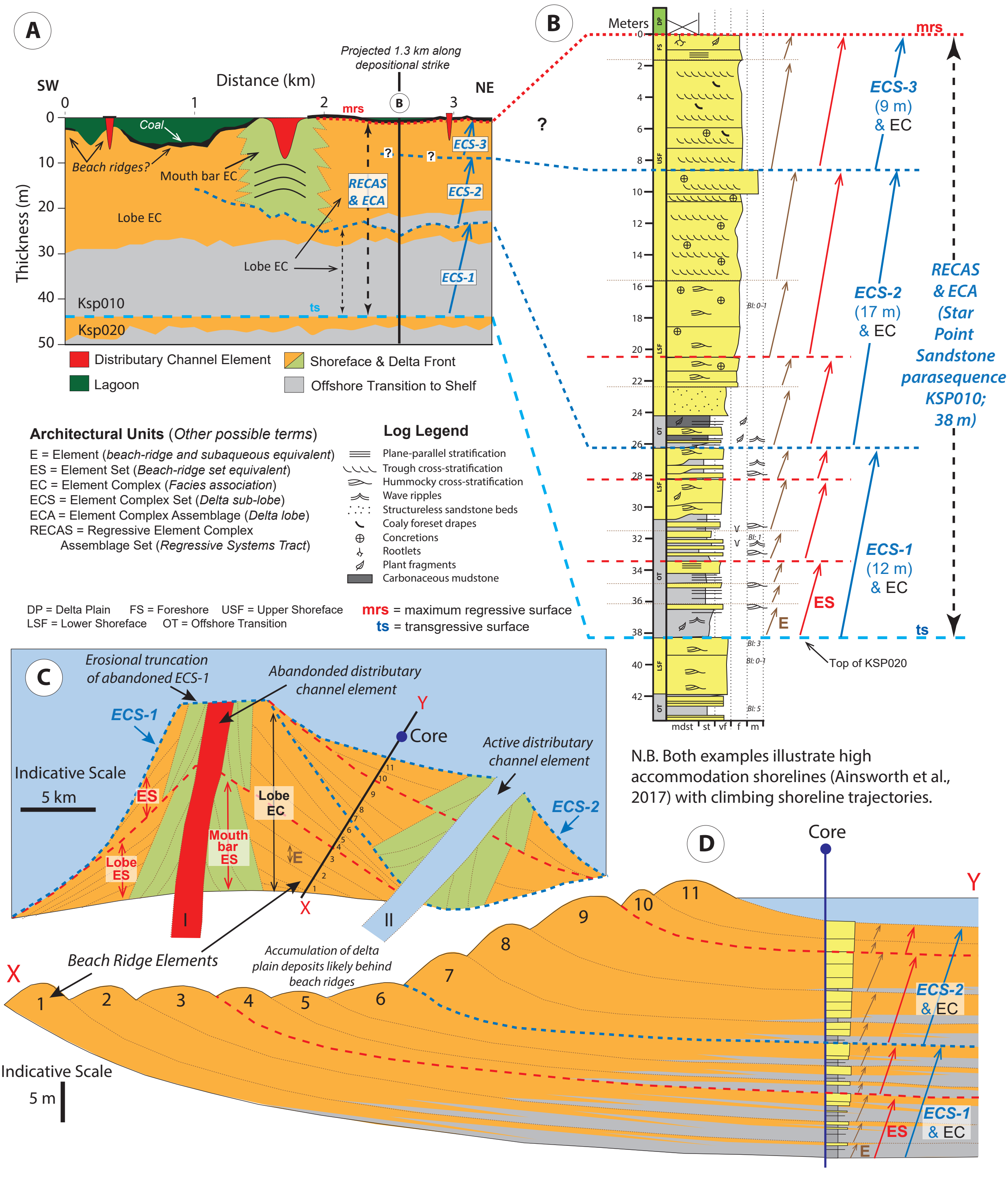
A
SW
Distance (km)
NE
Projected 1.3 km along depositional strike
mrs
Coal
Beach ridges?
Mouth bar EC
RECAS & ECA
ECS-3
ECS-2
ECS-1
Lobe EC
Ksp010
Ksp020
ts
Thickness (m)
Distributary Channel Element
Lagoon
Shoreface & Delta Front
Offshore Transition to Shelf
Architectural Units (Other possible terms)
E = Element (beach-ridge and subaqueous equivalent)
ES = Element Set (Beach-ridge set equivalent)
EC = Element Complex (Facies association)
ECS = Element Complex Set (Delta sub-lobe)
ECA = Element Complex Assemblage (Delta lobe)
RECAS = Regressive Element Complex Assemblage Set (Regressive Systems Tract)
Log Legend
Plane-parallel stratification
Trough cross-stratification
Hummocky cross-stratification
Wave ripples
Structureless sandstone beds
Coaly foreset drapes
Concretions
Rootlets
Plant fragments
Carbonaceous mudstone
DP = Delta Plain FS = Foreshore USF = Upper Shoreface
LSF = Lower Shoreface OT = Offshore Transition
mrs = maximum regressive surface
ts = transgressive surface
B
Meters
ECS-3 (9 m) & EC
ECS-2 (17 m) & EC
ECS-1 (12 m) & EC
RECAS & ECA (Star Point Sandstone parasequence KSP010; 38 m)
ES
E
Top of KSP020
mdst st vf f m
N.B. Both examples illustrate high accommodation shorelines (Ainsworth et al., 2017) with climbing shoreline trajectories.
C
Erosional truncation of abandoned ECS-1
Abandonded distributary channel element
Active distributary channel element
Indicative Scale
5 km
Lobe EC
Mouth bar ES
Lobe ES
Core
X
Y
Beach Ridge Elements
Accumulation of delta plain deposits likely behind beach ridges
D
Core
Indicative Scale
5 m
ECS-2 & EC
ECS-1 & EC

Fig. 7

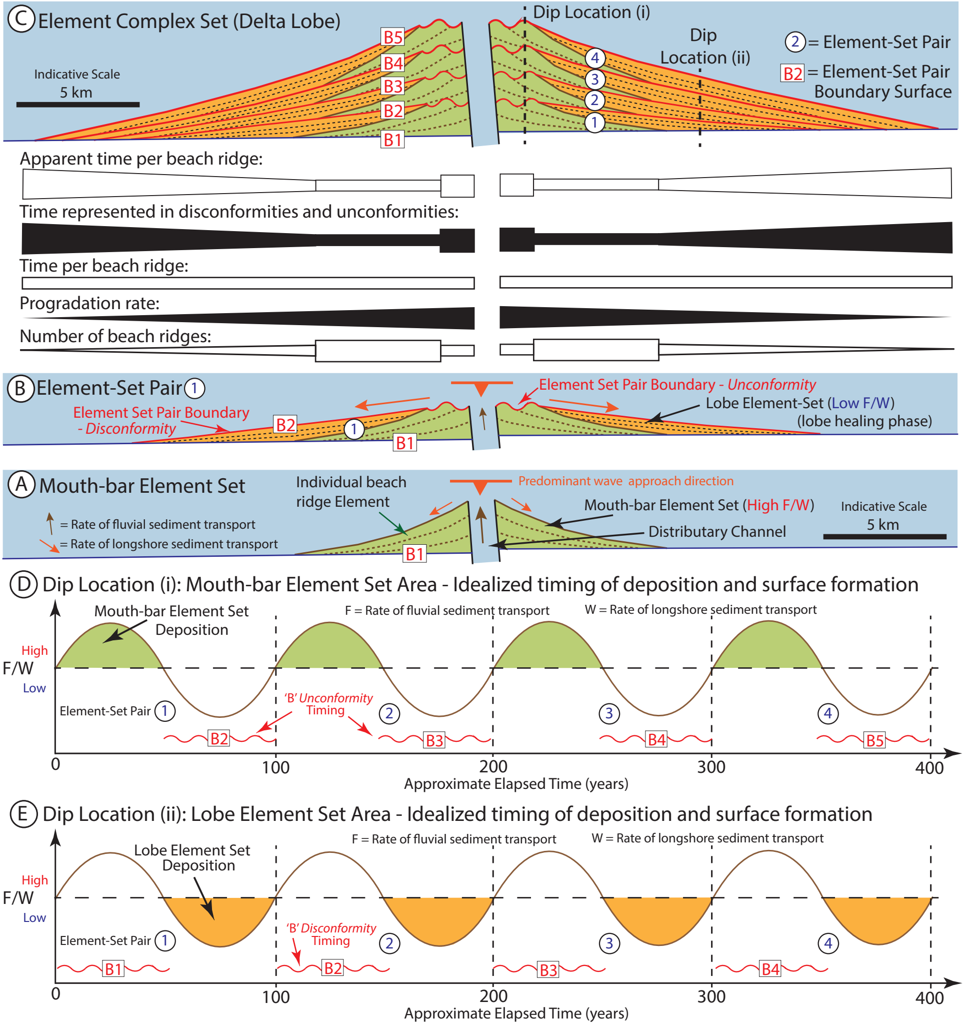

C Element Complex Set (Delta Lobe)
Indicative Scale
5 km
Dip Location (i)
Dip Location (ii)
2 = Element-Set Pair
B2 = Element-Set Pair Boundary Surface
B5
B4
B3
B2
B1
4
3
2
1
Apparent time per beach ridge:
Time represented in disconformities and unconformities:
Time per beach ridge:
Progradation rate:
Number of beach ridges:
B Element-Set Pair 1
Element Set Pair Boundary - Unconformity
Element Set Pair Boundary - Disconformity
Lobe Element-Set (Low F/W) (lobe healing phase)
A Mouth-bar Element Set
Individual beach ridge Element
Predominant wave approach direction
Mouth-bar Element Set (High F/W)
Distributary Channel
= Rate of fluvial sediment transport
= Rate of longshore sediment transport
Indicative Scale
5 km
D Dip Location (i): Mouth-bar Element Set Area - Idealized timing of deposition and surface formation
Mouth-bar Element Set Deposition
F = Rate of fluvial sediment transport
W = Rate of longshore sediment transport
High
F/W
Low
Element-Set Pair 1
'B' Unconformity Timing
B2
B3
B4
B5
0
100
200
300
400
Approximate Elapsed Time (years)
E Dip Location (ii): Lobe Element Set Area - Idealized timing of deposition and surface formation
Lobe Element Set Deposition
'B' Disconformity Timing
B1
B2
B3
B4
Approximate Elapsed Time (years)

Fig. 8

Ainsworth et al. (2018)

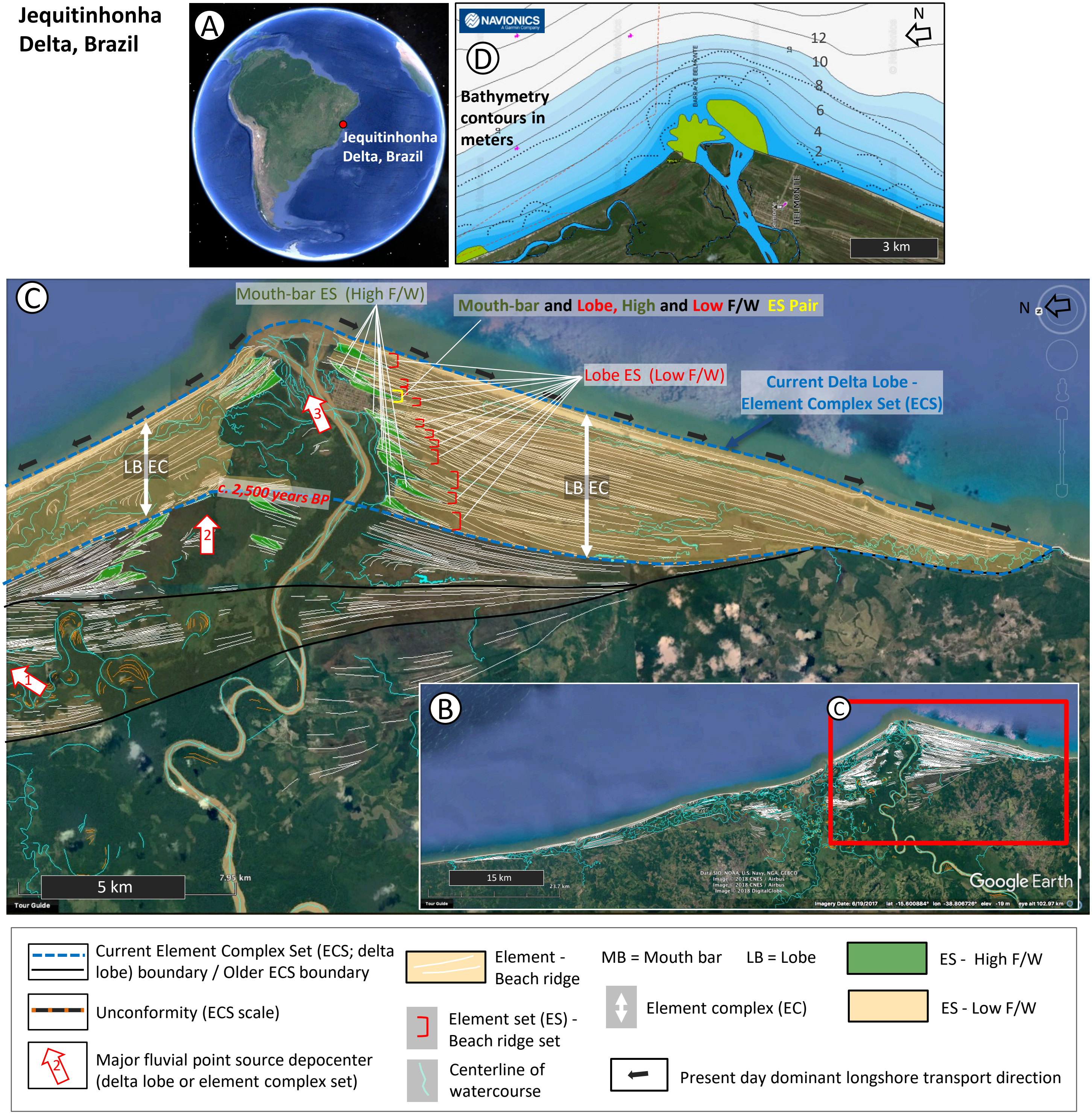

Fig. 9

Ainsworth et al. (2018)

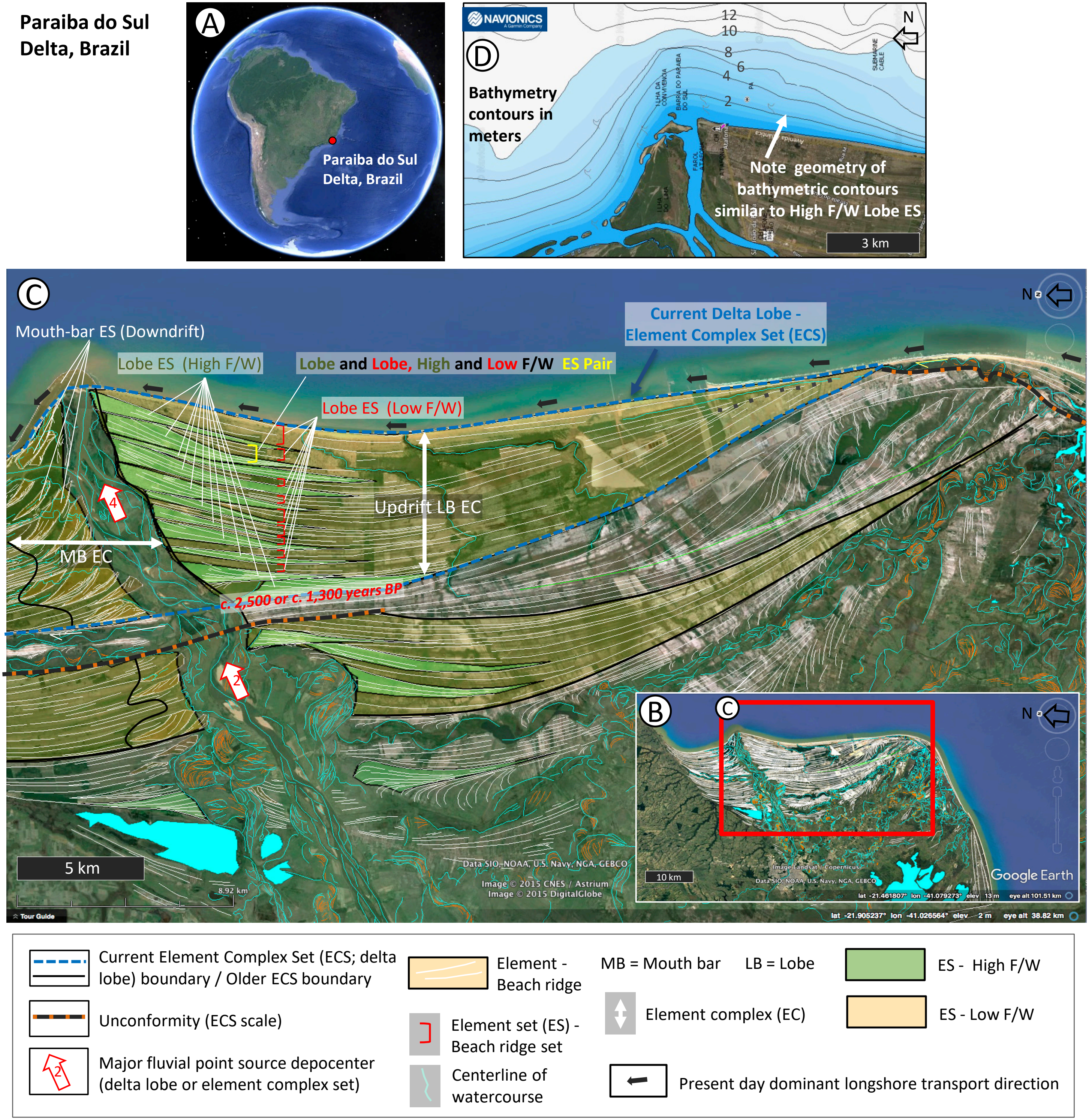

Fig. 10

Consistent and coherent plan and vertical section terms (*WAVE* Classification)	Equivalent plan section geomorphological terms	Equivalent vertical section stratigraphic terms	Comments
Element (e.g. lobe beach-ridge element); *E*	Beach ridge	Bedset – as used in this paper (see comments)	An element is represented by a genetically related thickening or thinning-upwards set of beds. This is descriptively termed a "bedset" in this paper and by Ainsworth et al. (2016, 2017).
Element Set (e.g. lobe beach-ridge element-set); *ES*	Beach-ridge set	*NA*	Also termed a bedset by some authors.
Element Set Pair (e.g. mouth-bar and lobe beach-ridge element-set pair); *ESP*	*NA*	*NA*	A new term introduced in this paper.
Element Complex (e.g. lobe element-complex, mouth-bar element-complex); *EC*	Mouth bar, updrift delta, down-drift delta	Facies Association	Facies associations in low accommodation systems (c.f. Ainsworth et al. 2017) have also been described as bedsets and parasequences (when bounded by flooding surfaces) by some authors.
Element Complex Set (e.g. Wf element-complex set); *ECS*	Delta lobe	Bedset (as previously applied in the Book Cliffs; e.g. Sømme et al. 2008). Parasequence (e.g. Bhattacharya and Walker, 1991; Pattison, 1995; Van Wagoner, 1995)	Note the multiple and confusing terms used for this level of architectural hierarchy in the literature. Also note that the "equivalent" terminology shown here is for wave-dominated systems only. Fluvial-dominated systems have been called another set of "lobe" terminology by multiple authors (e.g. Frazier, 1967).
Element Complex Assemblage (e.g. Wf element-complex-assemblage set); *ECA*	Delta	Parasequence. Parasequence Set.	In wave-dominated systems, this is commonly the whole delta (e.g. the Paraiba do Sul Delta; Fig. 10).
Regressive Element Complex Assemblage Set; *RECAS*	NA	Regressive Systems Tract (5th order). Parasequence Set.	Fifth order here represents timescales of 10^4 to 10^5 years.
Transgressive Element Complex Assemblage Set; *TECAS*	NA	Transgressive Systems Tract (5th order).	Fifth order here represents timescales of 10^4 to 10^5 years. Represented by a transgressive lag in low accommodation systems.
Regressive-Transgressive (full or partial shelf transit) Sequence; *RTS*.	NA	Parasequence (e.g. Mitchum and Van Wagoner, 1991; Ainsworth, 1994; Taylor and Lovell, 1995; Hampson, 2000). Fifth order, high-frequency Galloway sequence.	This level of hierarchy is the preferred level for the term "parasequence" (PS) when using the WAVE classification terminology (e.g. Ainsworth et al. 2018; this paper). The parasequence term is also used at this hierarchical level in the classical Book Cliffs papers (e.g. Hampson, 2000; Hampson et al. 2012).

TABLE 1. Comparison of WAVE Classification terms for both plan and vertical section stratigraphic units relevant to wave-dominated deltas (Vakarelov and Ainsworth, 2013; Ainsworth et al. 2017) with commonly used geomorphological terms for plan views and stratigraphic terms for vertical sections (see Figures 2 and 7). Note that many of the stratigraphic units have no common geomorphological term (column 2; NA = not applicable) or vertical section stratigraphic term (column 3) making correlation of plan view geometries to vertical section geometries problematical and prone to terminological misunderstandings and errors. Also note the common and confusing use of the terms "bedset", "parasequence" and "parasequence set" at two to three different vertical hierarchical scales (columns 3 and 4). The WAVE Classification (column 1) provides a consistent and coherent language for comparing plan section and vertical section stratigraphic architectures. Abbreviations of WAVE terms are shown in *italics* at the end of the descriptions in column 1.

Delta River Mouth. Current active ECS	Delta Classification (WAVE)	Climate Zone (Koppen-Geiger)	Catchment Area (km2)	Mean Spring Tidal Range (m)	ECS Duration (Years)	ECS Progradation Distance (m)	Minimum Progradation Rate (m per year)	# of ES pairs	Duration per ES pair (Years)	Dating Method	Source
Usumacinta–Grijalva (Mexico)	Wf Symmetrical	Tropical Monsoon	121,025	0.3	c. 970	7,000	7.2	10	c. 97	OSL & ^{14}C	Nooren et al. (2017)
Jequitinhonha (Brazil)	Wf Symmetrical	Tropical Wet	70,742	2.2	c. 2,500	8,000	3.2	11	c. 227	^{14}C	Martin et al. (1993)
Paraiba do Sul (Brazil)	Wf Asymmetrical	Tropical Savanna	57,085	1.3	c. 2,500	11,000	4.4	11	c. 227	^{14}C	Martin et al. (1993)
Paraiba do Sul (Brazil)	Wf Asymmetrical	Tropical Savanna	57,085	1.3	c. 1,300	11,000	8.5	11	c. 118	OSL	Vasconcelos et al. (2016)

TABLE 2. Data for three Holocene delta lobes (element complex sets; ECS). Note the duration of element set (ES) pairs for each delta is estimated at around 100 to 200 years. Data for the Paraiba do Sul from Martin et al. (1993) and Vasconcelos et al. (2016), the Jequitinhonha delta from Martin et al. (1993), and the Usumacinta–Grijalva delta from Nooren et al. (2017). ^{14}C = Carbon 14 absolute dating methods. OSL = optically stimulated luminescence absolute dating methods. N.B. absolute age durations have an uncertainty associated with the measurements (see details in relevant sources), hence they are stated as approximate durations (c. = circa).

Ainsworth et al. (2018)

Architectural Unit Name	Plan View (Geomorphology)	Rock Record (Vertical Section)	Probable Timeframe	Possible Response Type and Formative Mechanism
Bed	Lobate, sub-regional, km to multi-km-scale feature.	Bed: Single mm to cm scale bed in vertical section.	Hours to days per bed, but frequency of individual storm events may be seasonal or annual (months to years).	Autogenic: Fairweather wave activity, fluvial discharge fluctuations and individual storm events.
Element (E)	Beach Ridge: Single sub-regional beach ridge, km to multi-km-scale.	Bedset: A group of genetically related beds that can be arranged in an upward-thickening or upward-thinning trend. (decimeter- to meter-scale).	10s to 100s of years	Autogenic: Large (once in a decade-scale) storms can initiate new ridges. Fairweather and regular storm-related bed deposition are also part of the formative process.
Element Set (ES)	Beach Ridge Set: Multiple, grouped beach-ridges. Sub-regional, multi-km scale.	A group of genetically related bedsets (elements): Dominant normal progradation mode promotes vertical stacking of elements in offshore locations (meter scale).	100s of years	Allogenic: Part of a centennial-scale climate cycle influencing F/W at the coastline by changing river catchment precipitation and hence fluvial discharge, and/or wave power. The ES is either low or high F/W.
Element Set Pair	Two grouped beach ridge sets bounded by a disconformity or discontinuity. Sub-regional, multi-km scale.	A pair of genetically related element sets: Dominant normal progradation mode promotes lateral offset stacking of element set pairs in offshore locations (meter scale).	100s of years	Allogenic: A full centennial-scale climate cycle of high to low F/W at the coastline which alters river catchment precipitation and hence fluvial discharge, and/or wave power.
Element Complex Set (ECS)	Delta Lobe. Sub-regional, multi-km scale.	A group of genetically related element sets, element set pairs and element complexes (meter to decameter scale).	100s to 1000s of years	Autogenic: One river avulsion event on the delta plain.

TABLE 3. Description, probable timeframe of deposition and formative mechanism for architectural units on wave-dominated deltas.